

Original Research

Effect of Pore Structure of Supports on CO₂ Adsorption of Tetraethylenepentamine/Carbon Aerogels Prepared by Incipient Wetness Impregnation Method

Liang Chen¹, Mengdan Gong¹, Yan Cheng², Yongjun Liu^{1,3*}, Shi Yin¹, Deming Luo³

¹College of Architecture and Environment, Sichuan University, Chengdu, Sichuan, China

²Faculty of Geosciences and Environmental Engineering, Southwest Jiaotong University, Chengdu, Sichuan, China

³National Engineering Technology Research Center for Flue Gas Desulfurization, Chengdu, Sichuan, China

Received: 16 August 2018

Accepted: 16 October 2018

Abstract

Carbon aerogels (CA) with a wide range of pore parameters were synthesized through a sol-gel process and by varying the R/C mass ratios of initial mixtures. Tetraethylenepentamine (TEPA)/CA sorbents were prepared by incipient wetness impregnation method, which is more gentle, for CO₂ adsorption measurement. The results showed that the TEPA/CA sorbents displayed high CO₂ uptake up to 4.1 mmol/g at 75°C under 10% (v/v) CO₂/N₂ flow with fast adsorption and desorption kinetics. Larger pore volume instead of higher specific surface area of CA is beneficial for gas transfer into the pores of sorbents and good for CO₂ adsorption capacity of the sorbents. Moreover, a proper mesopore size (24.7 nm) of CA was found to be important in influencing CO₂ adsorption capacity of TEPA/CA sorbents. In addition to pore volume and pore size, it was found that the original surface morphology of CA plays a vital role in the CO₂ adsorption capacity of TEPA/CA sorbents as well by inducing CA treated by 3% nitric acid. The adsorption kinetics of sorbents were primarily influenced by the pore size of CA, namely that larger pore size (even over mesopore range) promotes the CO₂ diffusion inside the pores of sorbents. Insight into the role of porous support from this work could help in the further design of applicable and high-performance amine-modified sorbents.

Keywords: carbon aerogels; Tetraethylenepentamine; CO₂ adsorption; pore structure; adsorption kinetics

*e-mail: liuyj@scu.edu.cn

Introduction

The increasing concentration of CO₂ in the atmosphere produced by fossil fuels combustion is considered to be a main factor for global warming [1]. Carbon capture and storage (CCS) technology is a promising approach to reducing CO₂ emissions into the atmosphere for now [2]. The capture technology is the key to promoting CCS for capturing the low-level CO₂ (7 to 14% for coal-fired and as low as 4% for gas-fired [3]) from combustion flue gas. Post-combustion CO₂ capture is heavily studied because separating CO₂ at the exhaust of combustion allows for easy retrofit of already existing CO₂ sources. Amine-based technologies are currently considered the most advanced and cost-effective means for post-combustion CO₂ capture [4]. Although scrubbing by amine solution is the most mature technology for CO₂ capture, it results in serious problems such as high-energy consumption, solvent loss, and corrosion of process equipment. Adsorption by solid materials thus proposed an alternative, especially for the amine-modified sorbents, where amine-functionalities are dispersed inside the pores of a porous support, leading to enhanced CO₂ capture performance in diluted or high-content CO₂ condition.

Various porous materials (silica [5-9], carbon [10-12], metal organic framework [13, 14], metal oxides [15], polymers [16]) have been used to modify amine for CO₂ adsorption research. This research showed that the pore structure of support has a dominant impact on CO₂ adsorption performance of amine-modified sorbent. Besides, mesopores have been proven to play a vital role in CO₂ adsorption performance [11, 12, 17-19]. In the last decade, the pore structure of silica support influencing the CO₂ adsorption performance of amine-modified sorbent has been intensively investigated [6, 17, 19-26]. For example, Ahn's group have studied polyethyleneimine (PEI)-impregnated in a series of mesoporous silica materials and found that the CO₂ adsorption capacity and adsorption kinetics increased as a function of the pore diameter of the supports (2.8 to 6.0 nm) [21]. Yan's group studied PEI-impregnated SBA-15 supports and found that the relationship between CO₂ adsorption capacity and pore volume (rather than pore diameter) of the supports (0.71 to 1.14 cm³/g) are linearly related [24]. Feng et al. [6] prepared MCF with variable pore volume (1.54 to 2.04, window size (9.1 to 12.6 nm) and cell size (18.6 to 27.0 nm), and used MCF for Tetraethylenepentamine (TEPA) impregnated as sorbents to capture CO₂. The results showed that with increasing the pore volume and window size, as well as cell size of MCF, higher CO₂ adsorption capacity of sorbents could be obtained. Sayari et al. [23] studied PEI-impregnated mesoporous silica, including pore-expanded MCM-41, conventional SBA-15, and SBA-15 with platelet morphology. Under comparable conditions, the adsorption performance was found to be strongly dependent upon the length of pore channel (0.2 μm to 25 μm). These studies turned out the importance of pore

volume, pore size, pore length and three-dimensional structure property of supports in CO₂ uptake of amine-modified sorbents. Besides, the surface area positive related is also proposed [25].

Dissimilar to the silica support, the effect of carbon support's pore structure on CO₂ adsorption of amine-modified sorbents was studied by only a few groups. Song et al. [27] impregnated PEI onto the surface of several commercial active carbons with very high surface area (1121 to 2320 m²/g), variable pore volume (0.64 to 2.69 cm³/g) and pore size (2.22 to 7.26 nm), and carbon-based "molecular basket" sorbents for CO₂ capture obtained. The best support was the one with the highest pore volume and largest pore size, which lead to 3.06 mmol/g (75°C, pure CO₂) CO₂ adsorption capacity when loaded at 60% PEI. Furthermore, the research found that the meso-plus-macro-pore volume of carbon support plays a vital role in determining the CO₂ uptake of sorbents. Wang et al. [10] investigated the adsorption properties of PEI-impregnated mesoporous carbon (MC) (pore volume of 1.4 to 3.1 cm³/g) that were synthesized through a silica hard template-based approach. Higher CO₂ uptake of sorbent was obtained by impregnating a larger pore volume of MC. The effect of pore size on CO₂ adsorption performance was not investigated, which could be attributed to the possible reasons that the pore size distribution of MC is not highly concentrated and pore size range (10 to 20 nm) is too narrow.

Generally, amine-modified porous materials can be divided two ways: (i) wet impregnation and (ii) grafting. Both of them are easy to control the textural properties of the support because porous support preparation and amine-introduction steps are separate. Wet impregnation has been widely used for its obvious advantage in the simple and mild synthesis process, and getting high nitrogen content sorbent, which leads to a high CO₂ adsorption capacity. Sorbents of most research, including the aforementioned examples, were obtained by wet impregnation, the typical step of which was a long time of 0.5 to 12 h stirring of the mixture of support and dilute amine solution to evaporate volatile solvent since Xu et al. [28] prepared branched PEI-impregnated MCM-41 and found the good CO₂ adsorption performance of amine-modified sorbents. Branched PEI with high weight molecular was not easily entered into the pores of support. The longtime stirring might help PEI or other amine species coat on the surface of support as solvent is evaporated from the support/solvent mixture. While the longtime stirring to make amine homogeneous dispersed may destroy the shape of sorbent and make it a heap of slurry, which is not suitable for large-scale sorbent preparation and practical application. For example, using monolith support to prepare amine-impregnated sorbent, which requires the support of high mechanical strength, whereas porous carbon with large or ultra-large pore volume is generally delicate. Therefore, the more gentle impregnation methods need to choose.

Carbon aerogels (CA) is an important carbon material [29]. To the best of our knowledge, however, their pore structure impact on CO₂ adsorption was not systematically investigated. Wang's group investigated TEPA- and PEI-impregnated three different KOH/activated CA with various pore volumes (1.67 to 2.44 cm³/g) and pore sizes (5 to 6.33 nm), and found that the optimum support was the one with pore volume of 1.72 cm³/g and largest pore size (6.3 nm), which they ascribed to the larger pore size of support [30]. While the impacts of pore volume and KOH activation on CO₂ adsorption capacity and kinetics were not explicit, as well as the pore size range being too narrow.

In this work, TEPA was the chosen method for modifying CA due to its rich amino groups and low molecular weight, which makes it easy to reach all the pores. The TEPA/CA sorbents were prepared by incipient wetness impregnation, a conventional and simple but more gentle way. The study aims at investigating the effect of CA pore structure (pore volume, pore size) on amine loading, CO₂ adsorption, and kinetics of TEPA/CA sorbents through incipient wetness impregnation TEPA onto the surface of CA. A set of CA supports with different pore volumes and pore sizes were synthesized by varying the synthetic condition of resorcinol-formaldehyde (RF) sol-gels process. Besides, considering that the acid-treated process was widely used when synthesizing higher pore volume or pore size CA, for example, larger pore volume CA was obtained by the hard templating method, which was involved in acid etching [10], and to explore the influencing of acid treatment of CA on CO₂ adsorption as well, the nitric acid-activated CA was induced as a support for investigation. The CO₂ adsorption capacity, kinetics and regenerability of the TEPA/CA sorbents were studied. The influence of the pore parameters of the supports was discussed.

Materials and Methods

Sample Preparation

CA Supports

Carbon aerogels (CA) were synthesized by the polycondensation of resorcinol (R) and formaldehyde (F) using sodium carbonate (C) as a base catalyst. Resorcinol, formaldehyde aqueous solution and sodium carbonate were dissolved in distilled water, making the molar ratio of R: F: H₂O = 1:2:16.67 and the mass ratio of R:C ranged at 250 to 1000. The RF hydrogels were obtained by aging the above solution at room temperature for 24 h, 50°C for 24 h and 90°C for 72 h, respectively. After cooling, the hydrogels were immersed in an acetone bath to exchange water. RF aerogels were then by drying the acetone-exchanged RF hydrogels with supercritical carbon dioxide for 2 h. Finally, CA supports were obtained by calcination of

the RF aerogels at 900°C under N₂ atmosphere for 3 h with a ramping rate of 1.5°C/min. The produced carbon aerogels with different R/C mass ratio were denoted as CA_x, where x represents the value of R/C mass ratio. For the chemical activation process, sample CA was completely immersed into 3% wt nitric acid solution for 2 h at 60°C. After the sample was filtrated, it was washed using distilled water until the washing liquid became neutral, resulting in sample H-CA_x.

Sorbents

The TEPA/CA sorbents were prepared by incipient wetness impregnation method, where the desired concentration of TEPA ethanol solution was added into CA. The resultant wet slurry was dried at room temperature for 12 h, and then 60°C for 3 h. The obtained samples were denoted as CA_x-y or H-CA_x-y, where y represents the weight percentage of the TEPA in the sorbent.

Characterization

The laser Raman spectra were recorded using a HORIBA Jobin Yvon LabRAM HR Raman spectrometer (Paris, France) with a 30 mW Ar ion laser (532 nm). The morphology and microstructure of the adsorbents were investigated using a JMF-7500F electron microscope (JEOL Co., Japan) fixed with an Oxford INCA EDX detector system operating at 15 kV. Nitrogen adsorption-desorption isotherms were measured by AUTOSORB-IQ apparatus (Quantachrome Instruments, USA). CA Samples were degassed under vacuum for 6 h at 60°C and sorbents were for 3 h at 60°C before measurement. The specific surface area was calculated by the Brunauer-Emmett-Teller (BET) method, and the total pore volume was determined from the adsorption amount at a relative pressure of 0.99. The micropore volume was estimated using the Dubinin-Radushkevich (D-R) equation, and the mesopore volume was calculated by the difference between total pore volume and micropore volume. The mesopore size distribution was determined by the Barrett-Joyner-Halender (BJH) method using the desorption branch. Fourier transform infrared spectroscopy (FTIR) was performed by using a Nicolet 6700 (Thermo Electron Co., USA), in the range from 4000 to 400 cm⁻¹.

CO₂ Adsorption

CO₂ adsorption-desorption of the TEPA/CA sorbents was monitored using a thermal gravimetric analyzer (TGA, TA SDT600). In a typical adsorption process, about 10 mg of the sorbent was placed in a platinum sample pan. After being heated to 100°C in N₂ (200 mL/min) and held for 60 min, the sorbent was cooled down to the designed temperature and equilibrated at that temperature. The flow rate of N₂ was then switched to 180 mL/min and pure CO₂ (99.9%)

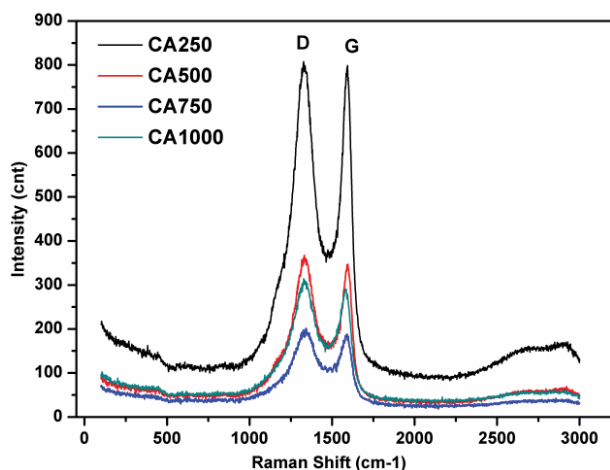


Fig. 1. Series of Raman spectra of the CA synthesized at various R/C mass ratio conditions.

with a rate of 20 mL/min was introduced. The sorbent was maintained in a 10% CO₂ steam for 30 min. For regenerability, cut the CO₂ stream and the flow rate of N₂ was switched back to 200 mL/min, and the sample was regenerated at the desired temperature (100, 75°C) after adsorption. The capacity of the sorbent (mmol/g) was calculated based on the weight gain of the sorbent during the adsorption.

Results and Discussion

Characterizing the Sorbents

Fig. 1 presents a series of Raman spectra of CA. The two peak, D band (around 1360 cm⁻¹) that was associated with the disordered structure and G band (around 1580 cm⁻¹) that was associated with the graphitic structure in the carbon are always observed in

most carbon and graphite materials [31]. With the R/C mass ratios increasing from 250 to 1000, the ratio of integrated intensities (I_G/I_D) remains unchanged, which reveals the ratios of disordered structure to the graphitic structure of CA to be at the same level [32].

The CA were synthesized by a sol-gel process with a controlled mass ratio of R/C, which affects the size of the clusters and the morphology of CA. The SEM images of the CA are shown in Fig. 2. Homogeneous but agglomerated spherical particles and compact structure of CA can be observed. The size of carbon particles varied with R/C mass ratio. The particle sizes for CA250, CA500, and CA750 are around 20 to 30 nm, 40 to 50 nm, and 50 to 60 nm, respectively. For CA1000 with higher R/C mass ratio of 1000, particles with a size close to 100 nm are discerned. It is clear that CA particle size becomes larger with the increasing R/C mass ratio. When the R/C mass ratio is low, namely the content of the catalyst is high and the density of nucleation center is high, and the cluster size is therefore small [33]. As the space between the particles forms interconnected pores of CA supports, by controlling the synthetic conditions of the sol-gel process, porous CA supports with similar pore structures, but different porosities were obtained. Sample H-CA1000, which was chemically activated with 3% nitric acid, retains the same particle-to-particle structure, but its surface seemed to become smooth because of acid etching. More details about CA will be further proven by the results of N₂ adsorption.

The SEM images of TEPA-modified CA1000 support with different amine loading are shown in Fig. 3. The sorbent with 50% TEPA displays an interconnected 3-D framework and shows similar morphology to the pristine CA1000, suggesting that TEPA was almost homogeneously distributed on the surface of CA particles by incipient wetness impregnation. With an increased TEPA loading of 60%, the particles become bigger and pore space is obviously reduced. When the

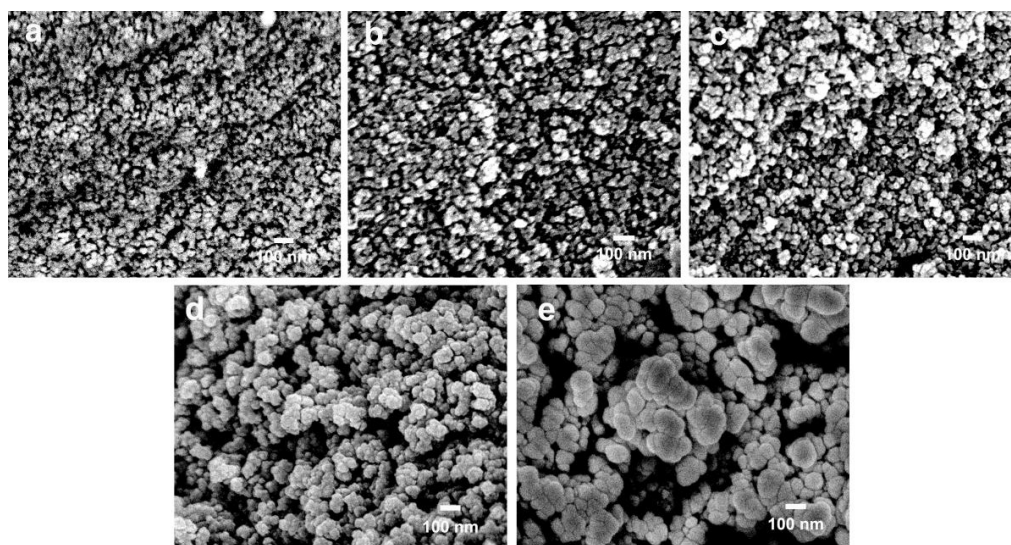


Fig. 2. SEM images of CA250 a), CA500 b), CA750 c), CA1000 d), and H-CA1000 e).

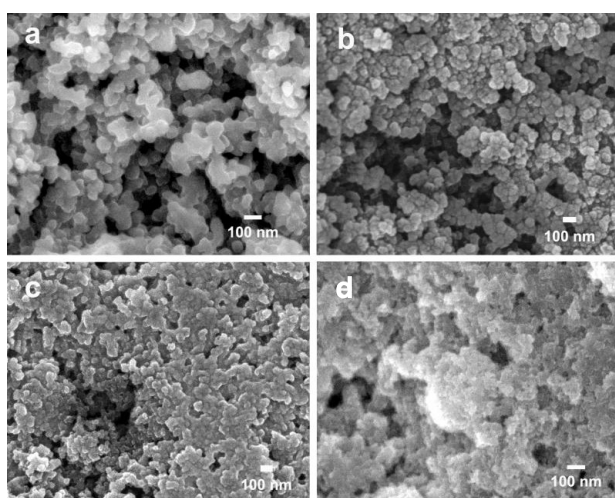


Fig. 3. SEM images of CA1000-50 a), CA1000-60 b), CA1000-70 c), and CA1000-80 d).

TEPA loading increased to 70%, most of the particles were connected by TEPA and formed into some solid block. With further increases of TEPA loading, this phenomenon becomes more serious, leading to the occupation of most pore space.

As shown in Fig. 4a), all CA supports displayed typical type IV N_2 sorption isotherms, and CA250, CA500, and CA750 with an H1 hysteresis loop indicate

a typical mesoporous structure of these materials. The sharp capillary condensation at a high-relative pressure of CA1000 compared to other CA supports indicated the presence of relatively large pores. As the supports were prepared under different synthetic conditions, the relative pressure at which the capillary condensation occurred shows a dependence on the R/C mass ratio value. Therefore, the mesoporosity of the support depends on the R/C ratio. The pore size of CA250, CA500 and CA750 most frequently occurred at 9.5 nm, 17.5 nm and 24.7 nm respectively, which is consistent with the SEM observations. CA1000 displayed a broad BJH pore diameter compared to other supports. The pore size distribution of H-CA1000 slightly shifted to a high pore size compared to CA1000 after acid activation. The detailed porosity parameters are summarized in Table 1. The BET surface area of CA ranges from 650 to 1185 m^2/g , while the total volume is about 1.22 to 3.16 cm^3/g . The detailed porosity parameters are summarized in Table 1. The specific surface area of H-CA1000 decreased to 650 m^2/g , which can be ascribed to the acid etching, even though CA1000 is treated by a low-concentration (3 wt%) nitric acid. The decreased pore volume of H-CA1000 (2.83 cm^3/g) could be explained by some pore-expanded pores beyond the N_2 sorption measurement.

From Fig. 4b), after TEPA impregnation, it is obvious that the N_2 sorption isotherms of CA1000-y also

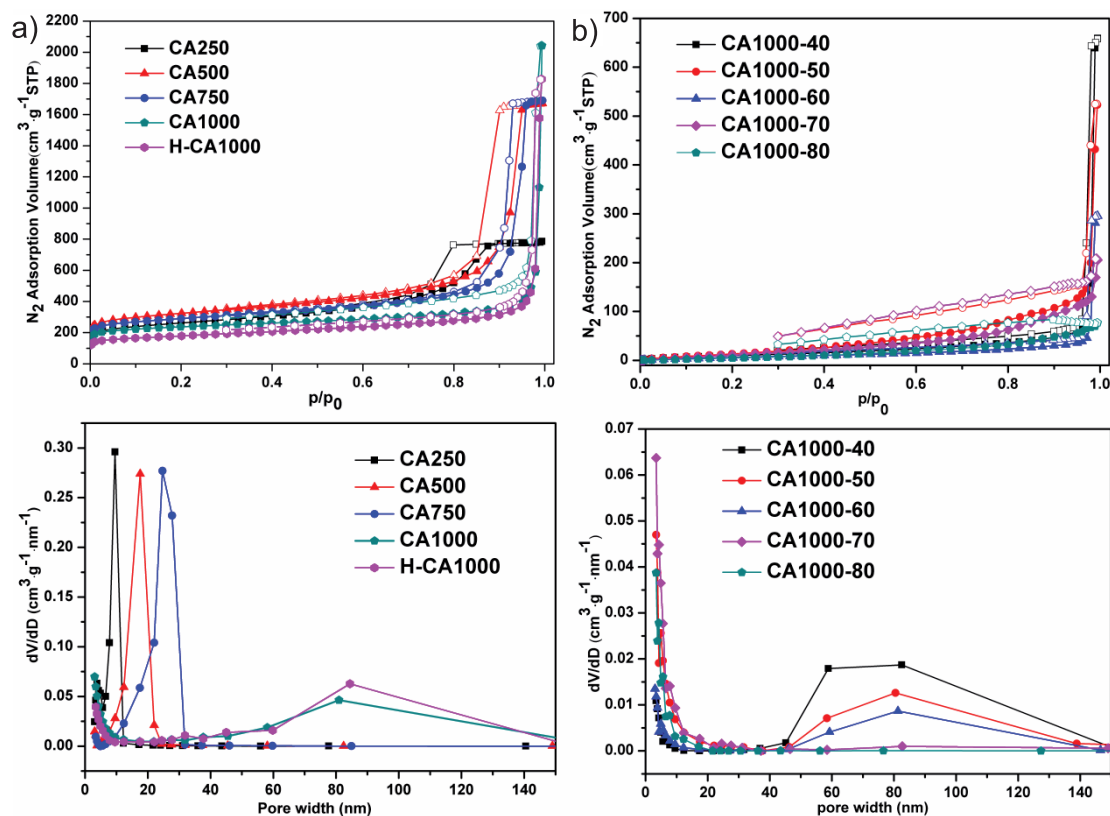


Fig. 4. 77k N_2 adsorption-desorption isotherms of CA supports: a) prepared under different synthetic conditions and CA1000 modified with TEPA b).

Table 1. Textural properties of CA supports and the amine-modified samples.

Sample	S_{BET} (m ² /g)	V_{total} (cm ³ /g)	V_{meso} (cm ³ /g)	V_{micro} (cm ³ /g)	D_p (nm) ^a	F_{meso} ^b
CA250	948	1.22	0.84	0.38	9.5	0.69
CA250-60	78	0.08	0.08	- ^c	-	1.00
CA500	1185	2.59	2.12	0.47	17.5	0.82
CA500-60	133	0.18	0.17	0.01	4.5	0.97
CA750	1069	2.61	2.19	0.42	24.7	0.84
CA750-60	37	0.30	0.30	-	22	1.00
CA1000	875	3.16	2.81	0.35	81	0.89
CA1000-40	45	1.02	1.01	0.01	58-82	0.99
CA1000-50	82	0.81	0.79	0.02	81	0.98
CA1000-60	34	0.46	0.45	0.01	81	0.99
CA1000-70	91	0.31	0.30	0.01	81	0.97
CA1000-80	38	0.10	0.10	-	-	1.00
H-CA1000	650	2.83	2.57	0.26	84	0.91
H-CA1000-70	74	0.23	0.22	0.01	84	0.96

^aThe peak of BJH pore diameter distribution

^bThe fraction of mesopore volume = mesopore volume/total volume

^cRepresents samples with negligible pore volumes and pore sizes because of pore plugging/pore filling

exhibit type IV. As expected, the values for the textural parameters of the CA1000-based sorbents, namely the BET surface area and pore volume, changed a lot, according to Table 1. For example, with a 40% TEPA impregnation, the surface area decreased from 875 to 45 m²/g and the total pore volume decreased from 3.16 to 1.02 cm³/g. It is also noticed that the micropore volume changed from 0.35 m³/g to almost zero (0.01 m³/g), suggesting the full filling or complete blockage of micropores by TEPA molecules even at a relatively low TEPA loading of 40%. Therefore, the

total pore volume of the amine-modified sorbent in the study is almost equal to its mesopore volumes. From TEPA loading of 40% to 80%, the pore volume of the sorbents shows a tendency of continuous decrease. At a high loading of 80%, almost all the pores were occupied, leading to a very low total volume of 0.10 cm³/g.

Fig. 5 shows the FT-IR spectra of CA1000, CA1000-70, H-CA1000 and H-CA1000-70 for comparison of the surface change of support after acid treatment and TEPA loading. The weak peak occurred at 1720 cm⁻¹ of H-CA1000 ascribed to C=O stretching, which confirmed that a few oxygenated surface groups were attached after nitric acid chemical activation [34]. After TEPA impregnation manifested peaks of TEPA occurred, which proved that TEPA was successfully introduced onto the surface of CA. The bands at 3293 and 1666 cm⁻¹ were assigned to symmetric stretching of primary amine (NH₂) and bending vibration of N-H from secondary amine (N(R)H), respectively [35, 36]. C-H stretching vibrations at peaks 2935, 2817 and 1446 cm⁻¹ [35]. The peaks at 1704 and 1361 cm⁻¹ could be associated to C=O stretching vibration, and O-H deformation vibration in carbamic acid stabilized from ammonium carbamate, which formed from the reaction between sorbent and trace of CO₂ from the air [9, 37]. The band at 1149 cm⁻¹ was related to the C-N stretching vibration peak [38].

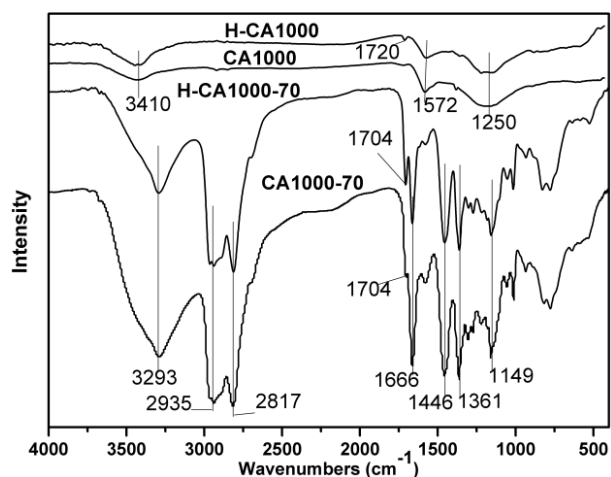


Fig. 5. FT-IR spectra of CA1000, CA1000-70, H-CA1000, and H-CA1000-70.

CO₂ Adsorption PerformanceEffect of Support Pore Structure on CO₂ Adsorption

The capacities at various amine loading weights were investigated on the sorbents prepared with different CA supports. As shown in Fig. 6, with the increase of amine loading, the CO₂ capacity shows a tendency to increase first and then decrease. CA1000 with 70% TEPA loading exhibited the highest capacity (4.10 mmol/g) among all the samples. For other CA-based sorbents, the maximum capacity reached 60% TEPA loading and decreased in order as follows: CA750-60 (3.65 mmol/g) > CA500-60 (2.28 mmol/g) > and CA250-60 (1.48 mmol/g). It seems that the capacity positively correlated with the total pore volume of the supports. Dissimilar to the pore volume, the larger specific area of CA support does not show positive promotion for the CO₂ adsorption capacity because CA1000 with the lowest specific area 872 m²/g among these CA supports but exhibited the highest capacity when loading 70% TEPA, as the specific area of a porous material can be largely contributed by micropores, which are more easily blocked during impregnation by amine than mesopore. This phenomenon indirectly proves that the mesopore or the mesopore portion in the total pore volume plays an important role in influencing CO₂ uptake capacity.

Furthermore, it is interesting to note that although the total pore volume of CA750 (2.61 cm³/g) nearly equals that of CA500 (2.59 cm³/g), the CO₂ adsorption capacity of CA750-60 (3.65 mmol/g) was obviously much higher than that of CA500-60 (2.28 mmol/g) under the same testing conditions. The biggest difference between the two supports exists only in the most frequently occurring pore sizes: CA750 (24.7 nm) and CA500 (17.5 nm). Therefore, it is probable that the TEPA enters CA750 more easily than in the case of CA500 through

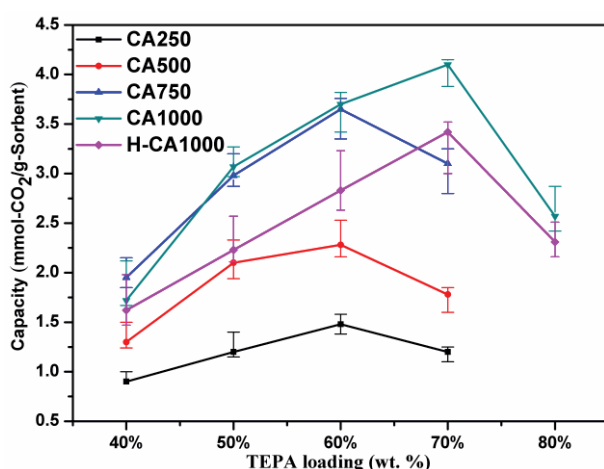


Fig. 6. Adsorption capacities of sorbents based on different CA supports at various amine loading weights by TG at 75°C in 10v% CO₂/N₂ mixture for 30 min.

impregnation, leading to fewer blockages of pores and better distribution of amine and thereby providing more space for gas diffusion and active sites for CO₂ adsorption. This is also partially supported by the larger residual pore volume of CA750-60 (0.30 cm³/g) than that of CA500-60 (0.18 cm³/g). This result revealed the importance of larger pore CA support aside from the mostly concerned pore volume of support.

The more finding is, at the same TEPA loading of 60%, despite CA1000 having a higher pore volume (3.16 cm³/g) and significantly larger pore size (beyond the mesopore size range) than CA750, no obvious increase in the capacity was observed. It seems that in this study an even larger pore size (>24.7 nm) did not help to improve the amine distribution, thereby enhancing CO₂ uptake. At higher TEPA loading of 70%, the capacity of CA1000-70 further increased, owing to a higher loading of amine, which provided more adsorptive sites since the CO₂ adsorption process of amine-modified sorbent was considered as the CO₂ molecular diffusion into the deep layers of amine [39, 40]. With even higher TEPA loading of 80%, the capacity of CA1000-80 dropped dramatically due to the excess amine blocking most pores, which resulted in insufficient space and interfacial area for CO₂ diffusion – as much other literature reported [10, 27]. Therefore, the capacity of CA750-70 dropped because CA750 with smaller pore volume cannot accommodate such more amine like CA1000.

Comparing the performance of H-CA1000-based sorbents provided insights into the roles of acid treatment of CA supports in influencing the CO₂ adsorption capacity of CA-based sorbents. It should be noticed that H-CA1000 with 2.83 cm³/g of pore volume and larger pore size (83 nm) showed much lower CO₂ uptake capacities than CA1000 and CA750 (pore volume of 2.61 cm³/g) after loading 40%, 50% and 60% TEPA. At the increasing loading weight of 70%, although the capacity of H-CA1000 (3.42 mmol/g) showed a slightly higher than CA750 because of its larger pore volume, the capacity of H-CA1000 is much lower than CA1000. As mentioned previously, the surface of CA suffering acid etching resulting in surface area decrease after 3% nitric acid treatment. Therefore, these results reveal that the important role of the original surface morphology of CA without acid treatment in CO₂ uptake of amine-impregnated CA sorbents. This implies that the preparation process of CA, which was related to acid treatment, should be taken into consideration when using CA as the support of amine-modified sorbent. For instance, higher pore volume CA or pore-expanded CA can be obtained by hard template routine that was removed by acid etching and oxide acid activation.

The dependence of adsorption capacities of sorbents CA1000-y with temperatures was also measured, as shown in Fig. 7. As agreed by most reports, the highest sorption capacities for the TEPA/CA sorbents were also observed at a mediated temperature of 75°C due to the compromise between adsorption thermodynamics and

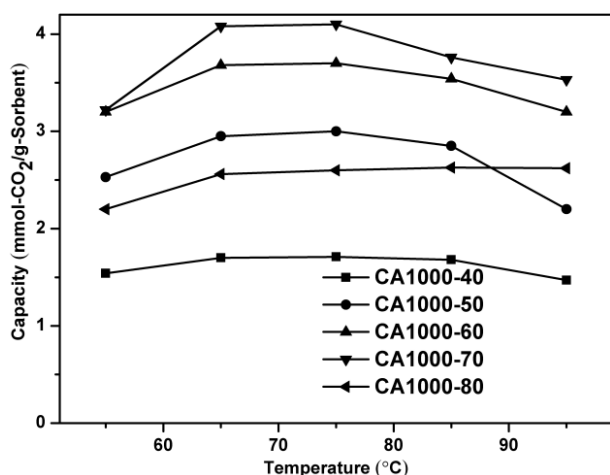


Fig. 7. Adsorption capacities of CA1000-y sorbents at various adsorption temperatures.

kinetic limitations [6]. However, only in the case of 1000-80 did the capacity show a continuous increase with the adsorption temperatures, indicating that the thermodynamic equilibrium of the sorbent had not yet been reached due to the existence of a large amount of amine functionalities. This result reflected that CO_2 diffusion into deep inner pores and/or into the TEPA films could be facilitated by increased adsorption temperature, but the capacity is still limited due to slow adsorption kinetics, which is largely governed by the support structure. Therefore, in order to further improve the capacity by utilization of more efficient support, except for the consideration of larger pore volume, a proper pore size of the structure could also be helpful.

Kinetics of CO_2 Adsorption

The adsorption kinetics of the TEPA-modified CA1000s was gravimetrically evaluated. Almost all the

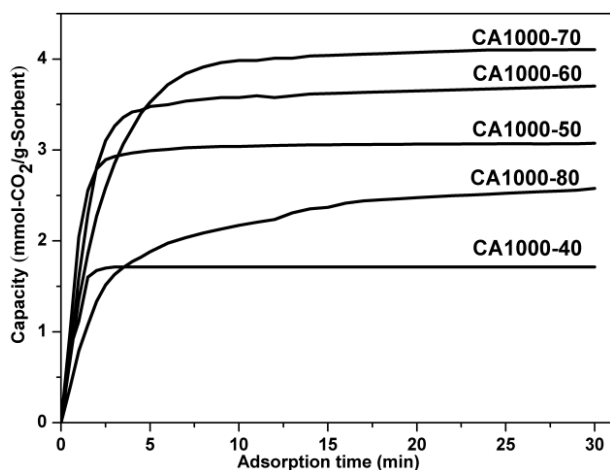


Fig. 8. Dynamic adsorption uptake curves of CA1000-y under adsorption conditions of 10% CO_2/N_2 gas, 75°C, 1 bar.

curves showed a sharp increase in the initial several minutes and reached a platform finally, as shown in Fig. 8. The slowdown can be observed more obviously in CA1000-70, reflecting higher diffusion resistance during the adsorption period for the sample with high amine loading. Although CA1000-70 showed higher capacity than all other samples, it showed much slower adsorption kinetics. In the case of CA1000-80, it shows even slower adsorption kinetics. Its CO_2 adsorption kept increasing slightly, indicating that the adsorption did not reach its thermodynamic equilibrium. So, despite more amine groups in the sorbents with high amine loadings, pore volume necessary for diffusion is reduced greatly. It could also be inferred that the interconnection of pores is partly blocked.

To clearly reveal the kinetics of CO_2 adsorption performance on TEPA/CA sorbents, the Avrami model was used to study the CO_2 adsorption kinetics of TEPA/CA sorbents. The Avrami model is based on simultaneous physical adsorption and chemical adsorption, which has been proven by other literature to be suitable for amine-modified sorbents [8, 41, 42]. It is presented by Eq 1:

$$q_t = q_e [1 - \exp(-k_a t)^{n_a}] \quad (1)$$

...where q_t and q_e represent the amount of CO_2 adsorbed at equilibrium and at a given point of time, respectively, in mmol/g; k_a is rate constant; and n_a refers to the index.

Fig. 9 shows that the Avrami model describes the experimental data of different sorbents well. Table 2 summarized the obtained parameters of the Avrami model. The high correlation coefficient ($R^2 > 98\%$, except CA250-60) indicates the good fitting by using this model. As expected, it could be seen that k_a increases with the R/C mass ratio of CA at the same 60% TEPA

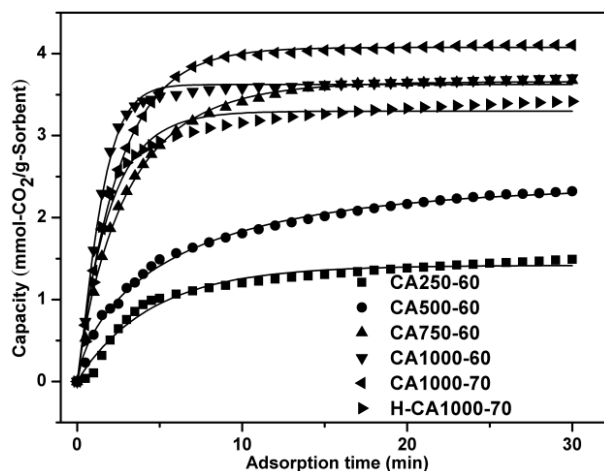


Fig. 9. Comparison of dynamic adsorption uptake curves of CAx-60, CA1000-70 and H-CA1000-70; adsorption conditions of 10% CO_2/N_2 gas, 75°C, 1 bar; scatters represent the experimental data and lines represent the fitting curve by using the Avrami model.

Table 2. Comparison of the obtained parameters of the Avrami model.

Sample	Adsorption capacity (mmol/g)	q_c (mmol/g)	k_a (1/min)	n_a	R^2
CA250-60	1.48	1.47	0.1600	0.7633	0.9764
CA500-60	2.28	2.40	0.1673	0.7031	0.9956
CA750-60	3.65	3.65	0.3278	0.8885	0.9987
CA1000-60	3.70	3.62	0.6555	1.2348	0.9954
CA1000-70	4.10	4.08	0.4000	0.9978	0.9995
H-CA1000-70	3.42	3.30	0.5134	0.9817	0.9820

loading weight because CA supports a larger pore volume and larger pore size, which promotes better diffusion of CO_2 gas inside the pores. This phenomenon agrees with the residual pore volumes of four sorbent orders: CA1000-60 ($0.45 \text{ cm}^3/\text{g}$) > CA750-60 ($0.30 \text{ cm}^3/\text{g}$) > CA500-60 ($0.17 \text{ cm}^3/\text{g}$) > CA250-60 ($0.08 \text{ cm}^3/\text{g}$). CA1000-70 showed a decreased k_a value compared to CA1000-60 because of more pores blocked by the added TEPA which increased the diffusion resistance. It should be noted that H-CA1000-70 ($k_a = 0.5134$) showed faster adsorption kinetics relative to CA1000-70 ($k_a = 0.4000$), although CA1000 with smaller pore volume than CA1000, which is ascribed to the larger pore size of H-CA1000. These results suggest that the large pore size (even over mesopore range) of CA was more beneficial to the kinetics of CO_2 uptake than pore volume.

Regeneration Performance

The stability and sorption rate of sorbent is a big concern for solid amine sorbents. Fig. 10 shows

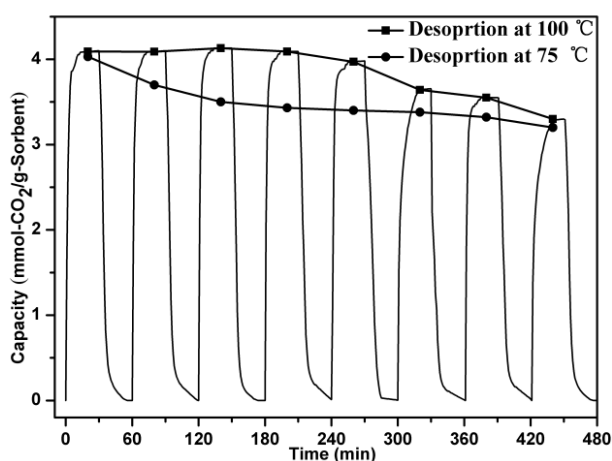


Fig. 10. Cyclic test of CA1000-70 using concentration sweeps at different desorption temperatures (CO_2 adsorption at 75°C for 30 min, desorption at 75°C or 100°C for 30 min); 10v% CO_2/N_2 mixture for adsorption and pure N_2 for initial activation/desorption were employed during the experiment, and the sorbent was desorbed in pure N_2 at 100°C for 60 min before the cyclic test.

the cyclic test of CA1000-70 in different desorption temperatures. At a desorption temperature of 100°C the desorption process was almost completed within 15 minutes, showing fast desorption kinetics. The CA1000-70 demonstrated a reversible and stable CO_2 adsorption-desorption performance in the first 5 repeated runs. However, after that, the capacity dropped gradually and the capacity of CA1000-70 was reduced to 3.30 mmol/g , namely 80% of the initial capacity after 8 runs. This is mainly due to the low thermal stability of TEPA leading to TEPA leaching as many others reported [7, 43]. To explore the lower temperature desorption for avoiding TEPA evaporation, the regeneration of the CA1000-70 test also carried out desorption at 75°C . The capacity of CA1000-70 dropped sharply in the first 3 runs. In the 4th cycle, the CO_2 uptake was only 3.40 mmol/g . This decrease may be due to the strong chemical interaction between TEPA and CO_2 , leading to the incomplete release of desorbed CO_2 at 75°C . But from cycle 4 to cycle 8, the capacity decreased slightly, where the CO_2 uptake is 3.20 mmol/g in cycle 8. This phenomenon reveals that a relatively low desorption temperature could avoid most of the volatilization and degradation of TEPA, but the long-term cycle drops the adsorption activity.

Conclusion

In this work, CA with similar interconnected structures but widely ranged textural properties were successfully synthesized by a sol-gel synthetic route and changing the R/C mass ratios. Pore-expanded CA support was obtained by 3% wt nitric acid treatment. TEPA was used to modify CA by using the incipient impregnation wetness method, a more gentle approach without long-time stirring; the results showed that obtained TEPA/CA sorbents are promising candidates for CO_2 adsorption and a deep study on the effect of the supports is significant as well.

It could be inferred that larger pore volume is beneficial for gas transfer into the pores of CA and therefore good for CO_2 uptake of the sorbents. Despite that, the mesopore size of CA (24.7 nm , in this study) was found to play a vital role in influencing the

CO₂ adsorption capacity of the TEPA/CA sorbents. The specific area of CA seems to show no obvious correlation with the CO₂ performance of the CA/TEPA sorbents, despite the higher specific area of support generally being desired for better amine dispersion and better mass transfer of CO₂. In addition to pore size and pore volume, the original surface morphology of CA without acid treatment also has a great impact on the CO₂ adsorption capacity of sorbents, which was inferred by the sharp CO₂ uptake decrease of nitric acid-activated CA. This phenomenon implies the importance of the CA support-preparing process (e.g., acid etching to remove the hard templates). The pore size of CA leads in CO₂ adsorption kinetics of sorbents, namely that increasing the pore size (even over mesopore range) improves the adsorption kinetics. Therefore, our work would provide new insight into the design and synthesis of high-performance amine-modified CA CO₂ sorbents.

Acknowledgments

This work was supported by the National Natural Science Foundation of China (No. 51406169).

Conflict of Interest

The authors declare no conflict of interest.

References

- YAUMI A.L., BAKAR M.Z.A., HAMEED B.H. Recent advances in functionalized composite solid materials for carbon dioxide capture. *Energy*. **124**, 461, **2017**.
- FIGUEROA J.D., FOUT T., PLASYNSKI S., MCILVRIED H., SRIVASTAVA R.D. Advances in CO₂ capture technology - The U.S. Department of Energy's Carbon Sequestration Program. *International Journal of Greenhouse Gas Control*. **2** (1), 9, **2008**.
- LEUNG D.Y.C., GARAMANNA G., MAROTO-VALER M.M. An overview of current status of carbon dioxide capture and storage technologies. *Renewable and Sustainable Energy Reviews*. **39**, 426, **2014**.
- PIRES J.C.M., MARTINS F.G., ALVIM-FERRAZ M.C.M., SIMÕES M. Recent developments on carbon capture and storage: An overview. *Chemical Engineering Research and Design*. **89** (9), 1446, **2011**.
- CHEN C., BHATTACHARJEE S. Trimodal nanoporous silica as a support for amine-based CO₂ adsorbents: Improvement in adsorption capacity and kinetics. *Applied Surface Science*. **396** (28), 1515, **2017**.
- FENG X., HU G., HU X., XIE G., XIE Y., LU J., LUO M. Tetraethylenepentamine-Modified Siliceous Mesocellular Foam (MCF) for CO₂ Capture. *Industrial & Engineering Chemistry Research*. **52** (11) 4221, **2013**.
- CHEN C., YANG S.T., AHN W.S., RYOO R. Amine-impregnated silica monolith with a hierarchical pore structure: enhancement of CO₂ capture capacity. *Chemical Communications*. **24**, 3627, **2009**.
- LIU Y., YU X. Carbon dioxide adsorption properties and adsorption/desorption kinetics of amine-functionalized KIT-6. *Applied Energy*. **211** (1), 1080, **2018**.
- DANON A., STAIR P.C., WEITZ E. FTIR Study of CO₂ Adsorption on Amine-Grafted SBA-15: Elucidation of Adsorbed Species. *The Journal of Physical Chemistry C*. **115** (23) 11540, **2011**.
- WANG J., WANG M., ZHAO B., QIAO W., LONG D., LING L. Mesoporous Carbon-Supported Solid Amine Sorbents for Low-Temperature Carbon Dioxide Capture. *Industrial & Engineering Chemistry Research*. **52** (15), 5437, **2013**.
- GIBSON J.A.A., GROMOV A.V., BRANDANI S., CAMPBELL E.E.B. The effect of pore structure on the CO₂ adsorption efficiency of polyamine impregnated porous carbons. *Microporous and Mesoporous Materials*. **208** (15), 129, **2015**.
- CHEN Z., DENG S., WEI H., WANG B., HUANG J., YU G. Polyethylenimine-impregnated resin for high CO₂ adsorption: an efficient adsorbent for CO₂ capture from simulated flue gas and ambient air. *ACS Applied Materials & Interfaces*. **5** (15) 6937, **2013**.
- SU X., BROMBERG L., MARTIS V., SIMEON F., HUQ A., HATTON T.A. Postsynthetic Functionalization of Mg-MOF-74 with Tetraethylenepentamine: Structural Characterization and Enhanced CO₂ Adsorption. *ACS Applied Materials & Interfaces*. **9** (12), 11299, **2017**.
- FLAIG R.W., OSBORN POPP T.M., FRACAROLI A.M., KAPUSTIN E.A., KALMUTZKI M.J., ALTAMIMI R.M., FATHIEH F., REIMER J.A., YAGHI O.M. The Chemistry of CO₂ Capture in an Amine-Functionalized Metal-Organic Framework under Dry and Humid Conditions. *Journal of the American Chemical Society*. **139** (35), 12125, **2017**.
- SONG F., ZHONG Q., DING J., ZHAO Y., BU Y. Mesoporous TiO₂ as the support of tetraethylenepentamine for CO₂ capture from simulated flue gas. *RSC Advances*. **3** (45) 23785, **2013**.
- LEE S., FILBURN T.P., GRAY M., PARK J.W., SONG H.J. Screening test of solid amine sorbents for CO₂ capture. *Industrial & Engineering Chemistry Research*. **47** (19) 7419, **2008**.
- HORI K., HIGUCHI T., AOKI Y., MIYAMOTO M., OUMI Y., YOGO K., UEMIYA S. Effect of pore size, aminosilane density and aminosilane molecular length on CO₂ adsorption performance in aminosilane modified mesoporous silica. *Microporous and Mesoporous Materials*. **246** (1), 158, **2017**.
- CHEN C., SON W.J., YOU K.S., AHN J.W., AHN W.S. Carbon dioxide capture using amine-impregnated HMS having textural mesoporosity. *Chemical Engineering Journal*. **161** (1-2), 46, **2010**.
- ZELEŇÁK V., BADANIČOVÁ M., HALAMOVÁ D., ČEJKA J., ZUKAL A., MURAFÁ N., GOERIGK G. Amine-modified ordered mesoporous silica: Effect of pore size on carbon dioxide capture. *Chemical Engineering Journal*. **144** (2), 336, **2008**.
- JAHANDAR LASHAKI M., SAYARI A. CO₂ capture using triamine-grafted SBA-15: The impact of the support pore structure. *Chemical Engineering Journal*. **334** (15), 1260, **2018**.
- SON W.J., CHOI J.S., AHN W.S. Adsorptive removal of carbon dioxide using polyethylenimine-loaded mesoporous silica materials. *Microporous and Mesoporous Materials*. **113** (1-3), 31, **2008**.

22. ZHANG H., GOEPPERT A., CZAUN M., PRAKASH G.K.S., OLAH G.A. CO₂ capture on easily regenerable hybrid adsorbents based on polyamines and mesocellular silica foam. Effect of pore volume of the support and polyamine molecular weight. *RSC Advances*. **4** (37) 19403, **2014**.
23. HEYDARI-GORJI A., YANG Y., SAYARI A. Effect of the Pore Length on CO₂ Adsorption over Amine-Modified Mesoporous Silicas. *Energy & Fuels*. **25** (9), 4206, **2011**.
24. YAN X., ZHANG L., ZHANG Y., YANG G., YAN Z. Amine-Modified SBA-15: Effect of Pore Structure on the Performance for CO₂ Capture. *Industrial & Engineering Chemistry Research*. **50** (6), 3220, **2011**.
25. YAN X., KOMARNENI S., YAN Z. CO₂ adsorption on Santa Barbara Amorphous-15 (SBA-15) and amine-modified Santa Barbara Amorphous-15 (SBA-15) with and without controlled microporosity. *Journal of Colloid and Interface Science*. **390** (1), 217, **2013**.
26. WANG D., WANG X., MA X., FILLERUP E., SONG C. Three-dimensional molecular basket sorbents for CO₂ capture: Effects of pore structure of supports and loading level of polyethylenimine. *Catalysis Today*. **233** (15), 100, **2014**.
27. WANG D., MA X., SENTORUN-SHALABY C., SONG C. Development of Carbon-Based "Molecular Basket" Sorbent for CO₂ Capture. *Industrial & Engineering Chemistry Research*. **51** (7), 3048, **2012**.
28. XU X., SONG C., ANDRÉSEN J.M., MILLER B.G., SCARONI A.W. Preparation and characterization of novel CO₂ "molecular basket" adsorbents based on polymer-modified mesoporous molecular sieve MCM-41. *Microporous and Mesoporous Materials*. **62** (1-2), 29, **2003**.
29. MALEKI H. Recent advances in aerogels for environmental remediation applications: A review. *Chemical Engineering Journal*. **300** (15), 98-118, **2016**.
30. XIE W., YU M., WANG R. CO₂ Capture Behaviors of Amine-Modified Resorcinol-Based Carbon Aerogels Adsorbents. *Aerosol and Air Quality Research*. **17**, 2715, **2017**.
31. MALDONADO-HÓDAR F.J., MORENO-CASTILLA C., RIVERA-UTRILLA J., HANZAWA Y., YAMADA Y. Catalytic Graphitization of Carbon Aerogels by Transition Metals. *Langmuir*. **16** (9), 4367, **2000**.
32. REYNOLDS G.A.M., FUNG A.W.P., WANG Z.H., DRESSELHAUS M.S., PEKALA R.W. The effects of external conditions on the internal structure of carbon aerogels. *Journal of Non-Crystalline Solids*. **188** (1-2), 27, **1995**.
33. AL-MUHTASEB S.A., RITTER J.A. Preparation and properties of resorcinol-formaldehyde organic and carbon gels. *Advanced Materials*. **15** (2), 101, **2003**.
34. GRZYB B., HILDENBRAND C., BERTHON-FABRY S., BÉGIN D., JOB N., RIGACCI A., ACHARD P. Functionalisation and chemical characterisation of cellulose-derived carbon aerogels. *Carbon*. **48** (8), 2297, **2010**.
35. SRIKANTH C.S., CHUANG S.S.C. Infrared Study of Strongly and Weakly Adsorbed CO₂ on Fresh and Oxidatively Degraded Amine Sorbents. *The Journal of Physical Chemistry C*. **117** (18), 9196, **2013**.
36. WANG X., CHEN L., GUO Q. Development of hybrid amine-functionalized MCM-41 sorbents for CO₂ capture. *Chemical Engineering Journal*. **260** (15), 573, **2015**.
37. HAHN M.W., JELIC J., BERGER E., REUTER K., JENTYS A., LERCHER J.A. Role of Amine Functionality for CO₂ Chemisorption on Silica. *The Journal of Physical Chemistry B*. **120** (8) 1988, **2016**.
38. LIU Q., SHI Y., ZHENG S., NING L., YE Q., TAO M., HE Y. Amine-functionalized low-cost industrial grade multi-walled carbon nanotubes for the capture of carbon dioxide. *Journal of Energy Chemistry*. **23** (1), 111, **2014**.
39. ZHAO J., SIMEON F., WANG Y., LUO G., HATTON T.A. Polyethylenimine-impregnated siliceous mesocellular foam particles as high capacity CO₂ adsorbents. *RSC Advances*. **2**, 6509, **2012**.
40. WANG X., SONG C. Temperature-programmed desorption of CO₂ from polyethylenimine-loaded SBA-15 as molecular basket sorbents. *Catalysis Today*, **194** (1), 44, **2012**.
41. LIU Q., SHI J., ZHENG S., TAO M., HE Y., SHI Y. Kinetics Studies of CO₂ Adsorption/Desorption on Amine-Functionalized Multiwalled Carbon Nanotubes. *Industrial & Engineering Chemistry Research*. **53** (29), 11677, **2014**.
42. ZHANG G., ZHAO P., HAO L., XU Y. Amine-modified SBA-15(P): A promising adsorbent for CO₂ capture. *Journal of CO₂ Utilization*. **24**, 22, **2018**.
43. WANG X., LI H., LIU H., HOU X. AS-synthesized mesoporous silica MSU-1 modified with tetraethylenepentamine for CO₂ adsorption. *Microporous and Mesoporous Materials*. **142** (2-3) 564, **2011**.